Development of a Method to Determine EDTA Concentration

A Major Qualifying Project Report

Submitted to the faculty of

WORCESTER POLYTECHNIC INSTITUTE

in partial fulfillment for the requirements for the

degree of Bachelor of Science

in Chemistry

by

Katherine P. Jones

Date:

5/2/2023

Project Advisor:

Professor Christopher Lambert

i. Abstract

Ethylenediaminetetraacetic acid (EDTA) is widely used in phlebotomy as an anticoagulant drug. There is a need for a simple, reliable, and cheap method to determine the concentration of EDTA in blood collection devices. This project is based on competition kinetics of fluorescence dyes (Rhodamine B, $Ru(bpy_3)^{2+}$, and Fluo-4FF), whose fluorescence intensities are altered [in] the presence of metal ions. In the presence of EDTA the metal ion is chelated and the change in the fluorescence is reversed. The sensitivity of the method is dependent on the relative binding constants of the metal ion with EDTA, the second order kinetics of fluorescence quenching by the metal ion and, in the case of Fluo-4FF the binding constant of the dye for calcium ions.

Table of Contents

ii. Acknowledgements

First and foremost, I would like to thank Professor Lambert for welcoming me to this project on very short notice. My completion of this project would not have been possible without his guidance and support over the last few months. I would like to thank my professors over the years in the CBC Department for teaching me everything I have needed to know to get to this point. Finally, I would like to thank my family and friends for supporting me throughout college, and especially over this whirlwind last semester.

iii. List of Tables

iii. List of Figures

1.0 Background

1.1 EDTA

Ethylenediaminetetraacetic acid, or EDTA, was first synthesized in the mid-1930s (George & Brady, 2006). It is an aminopolycarboxylic acid with the [molecular] formula $[CH_2N(CH_2CO_2H)_2]_2$. The structure of EDTA contains 2 amines and 4 carboxylates, as shown in Figure 1.

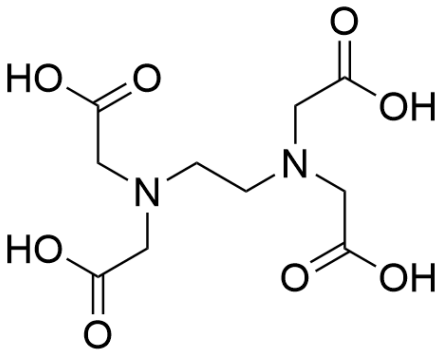

Figure 1: Structure of EDTA

At neutral pH, EDTA is deprotonated and acts as a hexadentate ligand, efficiently binding metal ions. The molecule's structure allows it to envelope these ions. EDTA forms strong, water-soluble metal complexes with Ca^{2+}, Fe^{2+}, and Fe^{3+}.

1.1.1 Uses of EDTA

EDTA has a variety of both pharmacological and non-nonpharmacological uses. It is most often used as an anticoagulant in phlebotomy, inhibiting clotting by removing calcium from the blood. In this treatment, EDTA forms water-soluble complexes with calcium in the bloodstream, which the body can eliminate in urine (George & Brady, 2006). EDTA can be used similarly for the

treatment of lead poisoning where the EDTA solubilizes the otherwise insoluble lead and allows it to be excreted. Because of its chelating ability, EDTA is sometimes used, although less commonly, for management of neurodegenerative diseases. Heavy metals in the blood stream can lead to the production of inflammatory agents, which negatively affect the nervous system. Inflammation can eventually lead to neurotoxicity. In these cases, EDTA is used to sequester heavy metals from the blood and excreted (George & Brady, 2022).

1.1.2 Detection of EDTA

Many variations on colorimetric detection of EDTA have been reported, some of which have been based on forming an EDTA-metal chelate and measuring the amount of this complex either directly or indirectly (dos Santos *et al*., 2023, Hamano *et al*., 1985). Others involve adding EDTA to a suitable metal complex and measuring the accompanying reduction in fluorescence upon addition (Bhattacharyya & Kundu, 1971). Often, these proposed methods require an extremely high pH, and are subject to interference from other ions in solution. Some previous studies on the detection and measurement of EDTA are summarized below.

Spectrophotometric determination of EDTA, Bhattacharyya, S. N., & Kundu, K. P. (1971).

Bhattacharyya and Kundu proposed a method that involved adding iron (III) to an EDTA solution and measuring the change in absorbance to determine EDTA, which has an absorption maximum 258 nm. Iron (III) was chosen because it has an absorption maximum at 304 nm, leading the authors to hypothesize that a method of direct measurement of the Fe-EDTA complex was possible. The experiment was carried out by adding ferric alum in sulfuric acid to an aliquot of EDTA and diluting these solutions in the concentration range of 10 – 70 μM. The absorption of the solutions was measured at 304 and 258 nm. The authors were successful in

measuring concentrations of EDTA as low as 10 μM. The presence of iron (II), however, could lead to interference and inaccurate results.

Sensitive spectrofluorimetric method for the determination of ethylenediaminetetraacetic acid and its salts in foods with zirconium ions and Alizarin Red S in a micellar medium. Campaña, A.M.G., Barrero, F.A., & Ceba, M.R. (1996).

Campaña *et al.* developed a method for detection of EDTA in foods such as mayonnaise and legumes based on the reaction of EDTA with Zr (IV) and Alizarin Red S, which produces a ternary complex. These reactants were combined and allowed to stand and reach total complexation. This complex is highly fluorescent at 600 nm when excited at 478 nm. Various micellar media solutions, including anionic SDS, cationic HTAB and CPC, and non-ionic TX-100, were added to the EDTA-Zr-Alizarin Red S solution. It was observed that upon addition of a cationic micellar medium (hexadecyltrimethylammonium bromide, in particular), the fluorescence emission of the ternary complex was approximately doubled. This allowed for spectrofluorimetric determination of the EDTA at a pH of 4.7. The detection limit was found to be 3.4 ng/ml.

Determination of EDTA in Aqueous Mediums. dos Santos, A.C., da Cunha, R., do Carmo Batista, W.V.F., de Fátima Gorgulho, H., & Benedini Martelli, P. (2023).

The basis of the method described in this paper is a colorimetric reaction, used to create an optimized spectrophotometric process for the determination of EDTA in aqueous medium. The reaction in use is that of EDTA, Zr (IV), and xylenol orange (XO) dye. Absorbance spectra of a solution containing 5 mL Zr (IV) and 5 mL XO dye were taken in the absence of EDTA. This initial solution showed an intense red color. As aliquots of EDTA were added to the Zr (IV)/XO

dye solution, the red color faded to yellow, and there was an accompanying reduction in absorbance. This method had a detection limit of 38 ng/L.

1.2 Kinetics

The rate of a reaction of reactants *A* and *B* is described by the formula

$$\upsilon = k[A]^{\alpha}[B]^{\beta}$$

where k is the rate constant, and α and β are experimentally determined values, called partial orders. The sum of all partial orders in a rate equation is called the overall order. (Laidler & Meiser, 1995).

1.2.1 Second order kinetics

In second order reactions, the sum of the exponents of reactants in the rate equation is equal to 2. Two possibilities for these reactions include one mechanism where the rate is proportional to the square root of the concentration of a reactant,

$$\upsilon = k[A]^2$$

where α is equal to 2, and one where the product of the concentrations of two reactants,

$$\upsilon = k[A][B]$$

where α and β are both equal to 1. The differential rate equation shows how the reaction rate changes with time, and the integral rate equation shows how concentration of species change over time. This mechanism will be discussed further in relation to Stern – Volmer kinetics.

1.2.2 Competition binding

The relative importance of binding constants and the kinetics of binding have been discussed in the literature (Jarmoskaite, *et al.* 2020). These authors looked at not only the magnitude of the binding constant but also the time required to for the equilibrium to be established. It is important to distinguish the association binding constant (K_a) from the dissociation constant (K_d). It is apparent that these are the reciprocal of each other *vide infra*.

$$K_d = \frac{1}{K_a}$$

The K_d value for calcium with EDTA changes slightly depending on the buffer but is typically on the order of 10 nM. For example, in TRIS buffer, the K_d for calcium EDTA value was found to be 5.05 nM, while in MOPS buffer, it is 4.26 nM, and in PIPES buffer it is 9.62 nM (Griko, 1999).

K_d is a constant used to measure the tendency of a molecule to separate (dissociate) into its lesser components. The simplest form of this reaction can be represented as

$$AB \rightleftharpoons A + B$$

From this equation, K_d can be calculated using

$$K_d = \frac{[A][B]}{[AB]}$$

K_a represents the reciprocal of K_d. It is the constant used to measure the tendency of two molecules to bind and form a larger complex. This reaction,

$$\rightleftharpoons$$

$$A + B \qquad AB$$

can be used to calculate K_a from

$$K_a = \frac{[AB]}{[A][B]}$$

For the purposes of this study, choosing dyes with appropriate K_a and K_d values was crucial. For the EDTA to successfully chelate the metal ion from the dye, the K_a of the dye with metal had to be less than that of the EDTA with the metal. Another way to view this is that the K_d of the metal and dye had to be greater than the K_a of the EDTA and dye. This allows the metal to have a greater tendency to leave the dye and bind with the EDTA. The ideal dye for this method should have a binding constant that is weaker than that of the EDTA with metal so that the EDTA can remove the metal ion from the dye. Using dyes of different affinities allows the measurement of EDTA in different concentration ranges.

1.3 Fluorescence

Fluorescence is the emission of a photon from an excited state. Typically, fluorescence occurs following absorption of a photon. Both absorption and emission are electronic transitions. Fluorescence involves a transition from the excited state [~~back~~] down to the ground state. Fluorescence occurs at a longer wavelength than absorbance and therefore at a lower energy.

The Jablonski diagram, shown in Figure 2, illustrates the processes involved in the absorption and emission of light.

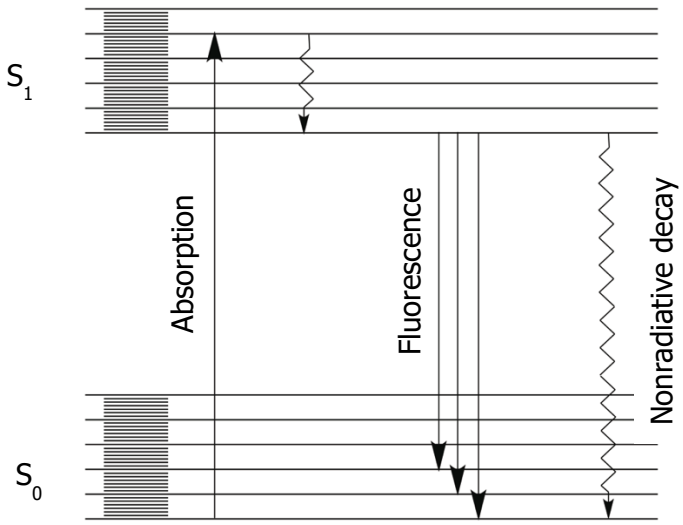

Figure 2: The Jablonski diagram

The intensity of fluorescence is a consequence of the intensity of the light absorbed, and the balance between nonradiative decay, where energy is lost as heat, and fluorescence. The wavelength (λ) of the absorption and that of the emission, is determined by the energy difference between the highest occupied molecular orbital (HOMO) and the lowest unoccupied molecular orbital (LUMO) based on Planck's relationship (Christie, 2017):

$$\Delta E = h\nu = hc/\lambda \qquad [1.1]$$

where h is Planck's constant, ν is frequency, c is the velocity of light and λ is the wavelength. The energy loss to due vibrational relaxation while in the excited state, and therefore, the shift to a longer wavelength, is called the Stokes shift. The inverse relationship between energy and wavelength explains why emission always occurs at a longer wavelength than absorption. The fact that the vibrational energy levels are similar in the ground and excited state for a rigid molecule explains why the fluorescence and emission spectra are mirror images of absorbance spectra.

1.3.1 Quantum yield and fluorescence lifetime

The quantum yield, (ϕ_F), is a measure of the efficiency of the fluorescence process. It is a ratio of photons emitted to photons absorbed, and the maximum quantum yield possible is 1.0. The intensity of a fluorescent signal is proportional to the amount of light absorbed, and the proportionality constant is the quantum yield, (*Fluorescence*, 2013).

The fluorescence lifetime of a substance is the length of time for which a fluorophore is in the excited state before it emits a photon. Because fluorescence is a random process, the lifetime is a measure of the average time spent in the excited state. Generally, fluorescence lifetimes last about 1 ns (Lakowicz, 2006), but can be calculated using the formula

$$\tau = \frac{1}{k_k + k_{nr}}$$

where k_r is the radiative rate constant and k_{nr} is a rate constant that groups all nonradiative decay processes.

Using the same nomenclature, the fluorescence quantum yield may be written:

$$\phi_F = \frac{k_r}{k_r + k_{nr}} = \frac{Number\ of\ photons\ emitted}{Number\ of\ photons\ absorbed}$$

1.3.2 Ion quenching of fluorescence

[The interaction of the excited state with another species may lead to the quenching of the fluorescence (Lakowicz, 2006). Quenching of the fluorescence (and the loss of excited state

energy) may occur by several mechanisms including energy transfer, electron transfer, chemical reaction, spin orbit coupling and intersystem crossing. Common quenchers include halogens, oxygen, amines, heavy metals and both oxidizing and reducing species. In the present work we initially looked at electron transfer processes with metal ions including copper and silver ions and subsequently looked at the possibility of fluorescence enhancement by controlling the balance between the non-radiative and radiative mechanisms of deactivation of the excited state.

1.3.3 Stern-Volmer quenching

The Stern-Volmer relationship is a method of determining the rate of the quenching of a fluorophore due to the presence of a quencher as a function of its concentration, taking into account the competition between radiative and nonradiative decay mechanisms (Gentleman, A.S. *et al.,* 2022). The fluorophore is deactivated due to an electron transfer between the fluorophore and quencher, returning to the ground state. The decrease in fluorescence intensity is described by the Stern-Volmer equation:

$$\frac{F_0}{F} = 1 + K[Q] = 1 + k_q \tau_0 [Q]$$

This relationship can be derived as follows (Albani, 2004):

In the presence of no quenching species, F^* can return from the excited state to the ground state by fluorescence:

$$F^* \xrightarrow{k_r} F + h\nu$$

and by nonradiative decay:

$$F^* \xrightarrow{k_{nr}} F$$

where k_1 and k_2 are the rate constants for these two processes. The equation for $[F^*]$ can be written as

$$\frac{[F^*]}{dt} = -(k_r + k_{nr})[F^*]$$

Integrating this equation gives

$$[F^*] = [F^*]_0 e^{-(k_r + k_{nr} + k_q[Q])/t}$$

and the fluorescence lifetime in the absence of a quencher is

$$\tau = \frac{1}{k_r + k_{nr}}$$

If a quencher, Q, is present, then a third mechanism to return F^* to the ground state is

$$F^* + Q \xrightarrow{k_q} F$$

where k_q is the bimolecular quenching constant. The rate equation for $[F^*]$ then becomes

$$\frac{[F^*]}{dt} = -(k_r + k_{nr} + k_q[Q])[F^*]$$

And the fluorescence lifetime in the presence of a quencher is given by

$$\tau_0 = \frac{1}{k_1 + k_2 + k_q[Q]}$$

Dividing τ_0 by τ yields

$$\frac{\tau_0}{\tau} = \frac{k_r + k_{nr} + k_q[Q]}{k_r + k_{nr}}$$

which can be simplified to the Stern-Volmer relationship:

$$\frac{\tau_0}{\tau} = 1 + K_{SV}[Q] = 1 + k_q \tau_0 [Q]$$

Here, K_{SV} is the Stern-Volmer quenching constant, which represents the sensitivity or vulnerability of the fluorophore to quenching. For example, a fluorophore in the center of a large macromolecule will likely have a low K_{SV} because it is largely inaccessible by the quencher,

while a free fluorophore in solution will have a much larger K_{SV} value (Lakowicz, 2006). A plot of $\frac{F_0}{F}$ versus $\tau_0[Q]$ (called a Stern-Volmer plot) should yield a straight line, the slope of which is K_{SV}.

1.3.3.1 Stern-Volmer kinetics

Fluorescence quenching may occur by several mechanisms including energy transfer, electron transfer, or by spin orbit coupling *vide supra*. The kinetics of the process is typically second order, involving the interaction of the quenching species with the excited state (Lakowicz, 2006). This process may be represented by

$$F^* + Q \xrightarrow{k_q} F + Q$$

where k_q is the bimolecular diffusion-controlled rate constant. In the absence of a quencher, the excited state decays by first order kinetics with a rate constant of k_d:

$$F^* \xrightarrow{k_d} F$$

[It should be noted that k_d here is the rate constant for all the inherent processes that lead to the deactivation of the excited state, i.e. $k_r + k_{nr}$. The overall rate for the deactivation of the excited state is given by:

$$-\frac{dF^*}{dt} = k_d[F^*] + k_q[F^*][Q]$$

The concentration of the excited state is typically on the order of nanomolar, and as such, the quencher concentration can be considered to be constant. The rate constant observed for the process is given by:

$$k_{obs} = k_d + k_q[Q]$$

From, this the fraction of excited state that undergo quenching can be calculated.

$$fraction\ quenched = \frac{k_q[Q]}{k_d + k_q[Q]}$$

If a fluorophore with a long lifetime (τ) is chosen, then the rate constant for inherent decay is small.

$$\tau = \frac{1}{k_d}$$

Therefore, species with a longer lifetime, and, consequently, a shorter k_d, should lead to a greater fraction of fluorescence being quenched.

1.3.4 Fluorescent dyes

An effective fluorescent dye is a compound that emits strongly in the visible region (Christie, 2017). There are some general principles based on the relationship between the structure of these dyes and their fluorescence intensity. Generally, fluorescent dyes are conjugated aromatic systems with multiple fused rings.

One important common feature of fluorescent dyes is structural rigidity. Rigid molecules minimize energy loss from excited states by intramolecular thermal motion and favor fluorescent emission over nonradiative energy loss. The “loose bolt effect” describes the decrease in fluorescence intensity by less rigid molecules (Christie, 2017). The presence of atoms with high atomic numbers, such as bromine or iodine, tends to reduce fluorescence in a process generally known as the heavy atom effect.

1.3.4.1 Rhodamine B

Rhodamines are a family of dyes and are a subset of triarylmethanes. Rhodamines contain a pyran ring, which leads to intense fluorescence due to the rigidity of the oxygen bridge. The intense red-violet fluorescence of the rhodamines makes them important in applications such as colorants, fluorescent markers, and photosensitizers. There are many members of the rhodamine family, but some of the most important are Rhodamine 6G, Rhodamine 123, and Rhodamine B. The structure of Rhodamine B is shown below in Figure 3.

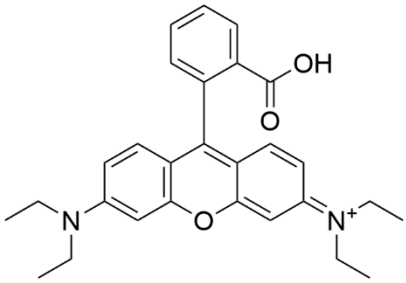

Figure 3: Molecular structure of Rhodamine B

Rhodamine B is used as a fluorochrome, fluorescent probe, or a histological dye. Practically, it is often employed as a paper dye, metal chelating agent, and in drugs and cosmetics (Christie, 2017). Although the dye has a relatively short fluorescence lifetime of about 1 ns (Kristoffersen *et al*., 2014), Rhodamine B was used initially as a model for our approach.

1.3.4.2 Tris(2,2'-bipyridyl)dichlororuthenium(II) hexahydrate

Tris(2,2′-bipyridyl)dichlororuthenium(II) hexahydrate (simplified formula: $[Ru(bpy)_3]^{2+}$ $2Cl^-$) is a red metal with polybipyridine structure, as shown in Figure 4. Fluorescence was first observed in $[Ru(bpy)_3]^{2+}$ in 1959 (Paris & Brandt, 1959). The dye is most commonly used as a catalyst in light-induced electron transfer reactions and is especially important in the photocatalyzed

splitting of water (Ryu *et al*., 2014). It also has applications in photochemistry, photovoltaics, and biosensors.

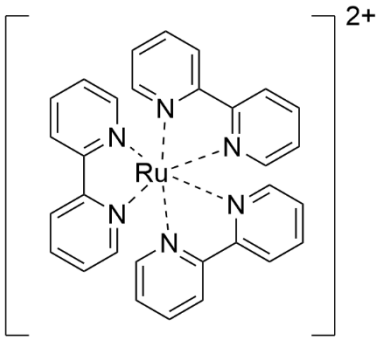

Figure 4: Molecular structure of $[Ru(bpy)_3]^{2+}$

Strong metal-ligand charge transfer (MLCT) absorption at 452 nm causes the orange color of $[Ru(bpy)_3]^{2+}$. The dye has a fluorescence lifetime of about 600 ns in water (Rusak *et al*., 2006). This long lifetime is due to the fact that the excited state is a triplet state, while the ground state is a singlet. Singlet-triplet transitions are often slow, as they are formally forbidden (Kalyanasundaram, 1982)

1.3.4.3 Fluo-4FF (2,2'-{[2-(2-{2-[Bis(carboxymethyl)amino]-5-(2,7-difluoro-6-hydroxy-3-oxo-3H-xanthen-9-yl)phenoxy}ethoxy)-4-methylphenyl]azanediyl}diacetic acid)

Fluo-4FF was the dye of choice for this project. Its photophysics and interactions with metal ions are based on the related compound Fluo-3. Fluo-3 was first synthesized and made commercially available by Molecular Probes in 1989 (*Fluo Calcium Indicators*, 2022). It is widely used in experiments on the photoactivation of caged chelators and belongs to a family of dyes that are specifically used for the detection of metal ions. The structure of Fluo-3 is shown below in Figure 5.

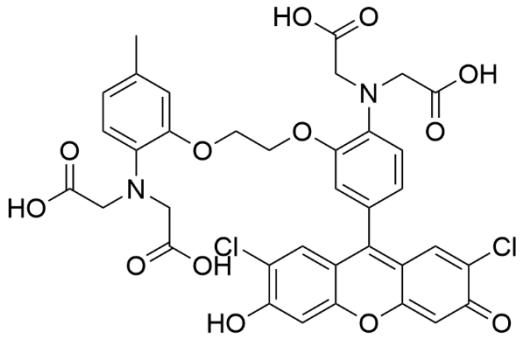

Figure 5: Structure of Fluo-3

Fluo fluorophores have been widely used for the detection of calcium ions. The dyes undergo an increase in fluorescence of at least 100-fold in the presence of the cation. (*Fluo Calcium Indicators*, 2022). This is believed to be due to increased rigidity of the molecule upon binding calcium. Since the fluorescence quantum yield is a balance between radiative and nonradiative decay, binding of the calcium ion causes the molecule to become significantly more rigid and, therefore, less able to undergo vibration, and hence, nonradiative decay. The unbound molecule exerts a portion of its energy through the movement of its carboxyl groups. As the carboxyl groups are deprotonated at pH 7 and bind calcium, they are effectively locked into place. The binding region of the molecule is outlined in red in Figure 6.

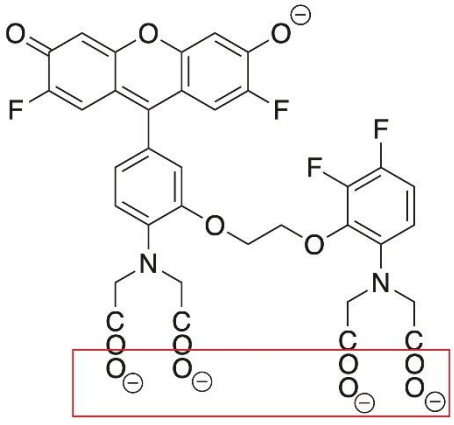

Figure 6: The molecular structure of deprotonated Fluo-4FF

Fluo-4 is an analog of Fluo-3 with the 2 chlorines replaced by fluorine. This results in an increased fluorescence excitation at 488 nm. Fluo-5F, Fluo-5N, and Fluo-4FF are analogs of Fluo-4, with lower Ca^{2+} binding affinities. Fluo-4FF has a k_d^{Ca2+} of 9.7 μM. The lower binding affinity allows for these analogs to detect Ca^{2+} levels in the range of 1 μM to 1 mM. These levels of Ca^{2+} may saturate Fluo-3 and Fluo-4 (Molecular Probes, 2022).

Fluo-4FF has excitation and emission wavelengths and 494 nm and 516 nm, respectively. It has a much lower binding affinity for Ca^{2+} than many other probes, making it suitable for the purpose of this experiment. Where Fluo-3 and Fluo-4 both have K_d values for Ca^{2+} of about 335 nM, the K_d of Fluo-4FF is 9.7 μM (*Fluo Calcium Indicators,* 2022). EDTA has the ability to effectively compete for the calcium since it has a K_d about 3 orders of magnitude smaller than the Fluo-4FF (Griko, 1999).

2.0 Methodology

2.1 Materials

Equipment:

- Perkin Elmer Lambda 35 UV/Vis Spectrometer
- Perkin Elmer FL6500 Fluorescence Spectrometer

Chemicals:

The names, formula, suppliers, and lot numbers for each chemical used are listed in Table 1.

Name	Formula	Supplier	Lot
Rhodamine B	$C_{28}H_{31}ClN_2O_3$	Alfa Aesar	D27Y023
Copper sulfate anhydrous	$CuSO_4$		3AC1207231A
Tris(2,2'-bipyridyl)dichlororuthenium(II) hexahydrate	$(C_{10}H_8N_2)_3RuCl_2 \cdot 6H_2O$	GFS Chemicals	M1
Silver nitrate	$AgNO_3$	EM	
Copper nitrate hemipentahydrate	$Cu(NO_3)_2 \cdot 2.5\ H_2O$	Alfa Aesar	10167841
Ethylenediaminetetraacetic acid (EDTA)	$C_{10}H_{16}N_2O_8$	Aldrich	00611LQ
Magnesium chloride	$MgCl_2$	Aldrich	05524JI
Iron (II) chloride hydrate	$FeCl_2 \cdot H_2O$	Alfa Aesar	H10Y019
Sodium EDTA dihydrate	$C_{10}H_{12}N_2O_8Na \cdot 2H_2O$	Sigma	11K0270
Lithium acetate	CH_3CO_2Li	Aldrich	10019887
Fluo-4FF pentapotassium salt	$C_{35}H_{21}O_{13}N_2F_4K_5$	Thermo-Fisher	2533869

Table 1: Name, formula, supplier, and the Lot Number of each chemical used

2.2 Methods

2.2.1 Rhodamine B

Determining the molar absorption coefficient

Typical solutions were prepared by making a stock solution of Rhodamine B in deionized water (9.979 mM) and diluting this ten times. Specific concentrations of Rhodamine B were then prepared from this diluted sample and are given in Table 2.

Solution	**[Rhodamine B] (mM)**
Stock	9.979
Dilution 1	0.9978
Dilution 2	0.09951
Dilution 3	0.02488
Dilution 4	0.03732
Dilution 5	0.04976
Dilution 6	0.06219
Dilution 7	0.07463
Dilution 8	0.009933

Table 2: Concentration of Rhodamine B in each solution

The absorbance of each sample was then measured between 350 and 800 nm. The measurements from samples with an optical density of approximately 1 or less were then used to create a Beer-Lambert plot. Using the Beer-Lambert relation, the molar absorption coefficient was determined.

Measuring fluorescence quenching by $CuSO_4$

The fluorescence of the 0.09978 mM Rhodamine B solution (the highest concentration of the samples used to construct the Beer-Lambert plot) was measured between 520 and 750 nm, and the maximum value was recorded. 0.0131 g $CuSO_4$ were then dissolved in 100 mL of the Rhodamine B to create a solution that was 8.18 mM in $CuSO_4$. The fluorescence of this solution

was measured in the same range, and the decrease in peak intensity was recorded. An additional 0.0450 g of $CuSO_4$ were then added to the solution for a final concentration of 36.23 mM $CuSO_4$. This relatively large amount of $CuSO_4$ was added in an attempt to measure the maximum quenching ability of the Cu^{2+}. The fluorescence was measured a final time in the same range, and the peak intensity was recorded. A graph of this data was made, plotting the fluorescence intensity versus the concentration of $CuSO_4$.

2.2.2 Tris(2,2'-bipyridyl)dichlororuthenium(II) hexahydrate

Comparison of fluorescence quenching of five metals

Five different metal ions ($Mg^{2+,}$ Fe (II), Cu (II), Li^+, and Ag (I)) were tested in order to find one that could most effectively quench the fluorescence of $[Ru(bpy)_3]^{2+}$. To begin, five metal ion-containing complexes were measured and added into separate 25 mL volumetric flasks. Each flask contained enough of the complex to give an approximate concentration of 10 mM. The exact concentrations are listed in Table 3. Each solid was then dissolved in 25 mL of 0.1 mM $[Ru(bpy)_3]^{2+}$ $2Cl^-$ solution.

Metal Complex	Concentration (mM)
$MgCl_2$	9.97
$FeCl_2 \cdot H_2O$	9.78
$Cu(NO_3)_2$	9.92
CH_3CO_2Li	10.3
$AgNO_3$	10.3

Table 3: Exact concentrations of metal ion solutions

First, the fluorescence of a sample of the $[Ru(bpy)_3]^{2+}$ solution before the addition of any metal was measured between 450-750 nm. The peak intensity was recorded as a baseline. The fluorescence intensities of each of the metal ion solutions were then measured, and their peak

values were recorded. These five values were compared to the initial fluorescence of the $[Ru(bpy)_3]^{2+}$ to evaluate most effective quenchers.

Of the five metals tested, Fe (II) and Ag (I) successfully quenched the fluorescence of the $[Ru(bpy)_3]^{2+}$. The next step was to test whether the ions could be removed from the $[Ru(bpy)_3]^{2+}$ by EDTA. A solution of 9.82 mM EDTA was prepared in 25 mL of 0.1 mM $[Ru(bpy)_3]^{2+}$. 1 mL of this solution, along with 1 mL of the $[Ru(bpy)_3]^{2+}$ solution, and 1 mL of the $AgNO_3$ solution were added to a fluorescence cuvette. Another cuvette was prepared in the same manner, substituting $FeCl_2$ for the $AgNO_3$. The fluorescence of each sample was measured, again between 450-750 nm, and the peak intensities were recorded. The fluorescence intensities of both samples were compared to their respective intensities before the addition of EDTA. $AgNO_3$ appeared to be successfully chelated by the EDTA, so it was chosen for further evaluation.

Investigating EDTA's ability to chelate $AgNO_3$

The previous experiment revealed the potential of $[Ru(bpy)_3]^{2+}$ and $AgNO_3$ as a fluorophore-quencher pair that could be separated by EDTA. The goal of the following experiments was to investigate this combination in greater detail.

The first part of this experiment focuses on the reaction between $[Ru(bpy)_3]^{2+}$ and $AgNO_3$. The following solutions were prepared using pH 7.2 KH_2PO_4 buffer in an attempt to mitigate any interference due to acidic deionized water:

Solution A: 0.09367 mM $[Ru(bpy)_3]^{2+}$ $2Cl^-$

Solution B: 0.09367 mM $[Ru(bpy)_3]^{2+}$ $2Cl^-$, 0.09925 M $AgNO_3$

The fluorescence and absorbance of solutions A and B was measured and recorded. Next, 3.0 mL of solution A were added to a cuvette along with 20.0 μL of solution B, and the fluorescence and

absorbance of the resulting sample was measured. This process, including the addition of a 20.0 uL aliquot of solution B to the cuvette and measuring the fluorescence and absorbance of the sample, was repeated 4 more times. In total, 100 μL of solution B were added to the cuvette. The concentration of $AgNO_3$ in each sampled is listed in Table 4.

Solution	**[$AgNO_3$] (mM)**
Pure A	0
3 mL A + 20 μL B	0.663
3 mL A + 40 μL B	1.323
3 mL A + 60 μL B	1.987
3 mL A + 80 uL B	2.647
3 mL A + 100 μL B	3.308
Pure B	100

Table 4: Concentration of AgNO3 in each [Ru(bpy)3]2+ solution

Two graphs of the data from this experiment were made, with one showing fluorescence intensity versus the concentration of $AgNO_3$, and the other showing absorbance versus the concentration of $AgNO_3$.

The second part of this experiment focuses on the interactions between $[Ru(bpy)_3]^{2+}$, $AgNO_3$, and EDTA. The following solutions were prepared in pH 7.2 KH_2PO_4 buffer:

Solution C: 0.1015 mM $[Ru(bpy)_3]^{2+}$ $2Cl^-$, 2.97 mM $AgNO_3$

Solution D: 0.1015 mM $[Ru(bpy)_3]^{2+}$ $2Cl^-$, 2.97 mM $AgNO_3$, 0.01 M EDTA

The fluorescence and absorbance of solutions C and D were measured and recorded. Next, 2.0 mL of solution C were added to a cuvette along with 150 μL of solution D. The fluorescence and absorbance of this sample were measured. The process of adding a 150 μL aliquot of solution D to the cuvette and measuring the fluorescence and absorbance of the resulting solution

was repeated 9 more times. The concentration of EDTA is each solution is listed in Table 5. Two graphs were made using the data from this experiment, with one showing fluorescence intensity versus EDTA concentration, and the other showing absorbance versus EDTA concentration.

Solution	[EDTA] (mM)
Pure C	0
2 mL C + 150 µL D	0.75
2 mL C + 300 µL D	1.50
2 mL C + 450 µL D	2.25
2 mL C + 600 µL D	3.00
2 mL C + 750 µL D	3.75
2 mL C + 900 µL D	4.50
2 mL C + 1050 µL D	5.25
2 mL C + 1200 µL D	6.00
2 mL C + 1350 µL D	6.75
2 mL C + 1500 µL D	7.50
Pure D	10

Table 5: Concentration of EDTA in each $AgNO_3$ and $[Ru(bpy)_3]^{2+}2Cl^-$ solution

2.2.3 Fluo-4FF

1 mL of pH 7.2 KH_2PO_4 buffer was added to the 500 µg sample of Fluo-4FF. 20 µL of this solution was added to a cuvette along with 3 mL of buffer for a final Fluo-4FF concentration of 1.74×10^{-7} mM. The fluorescence and absorbance of this sample was measured and recorded. Next, in preparation to investigate the effect Ca^{2+} had on the dye, a 0.9101 mM solution of $CaCl_2$ was made. 10 µL of this was added to the cuvette already containing Fluo-4FF and buffer, and the fluorescence of the sample was measured. Three additional aliquots of varied volumes (20 µL, 30 µL, and 240 µL) were added to the cuvette, and the fluorescence of the samples were measured after each addition. The concentration on $CaCl_2$ is each solution is detailed in Table 6.

Volume $CaCl_2$ (µL)	[$CaCl_2$] (mM)
0	0
10	0.003023588
30	0.009010891
60	0.017845098
300	0.082736364

Table 6: Concentration of $CaCl_2$ in each solution of Fluo-4FF

300 µL of 10 mM EDTA were added to the sample, and the fluorescence intensity was measured and recorded.

3.0 Results

3.1 Rhodamine B

The absorption spectra of Rhodamine B as a function of concentration are shown in Figure 7.

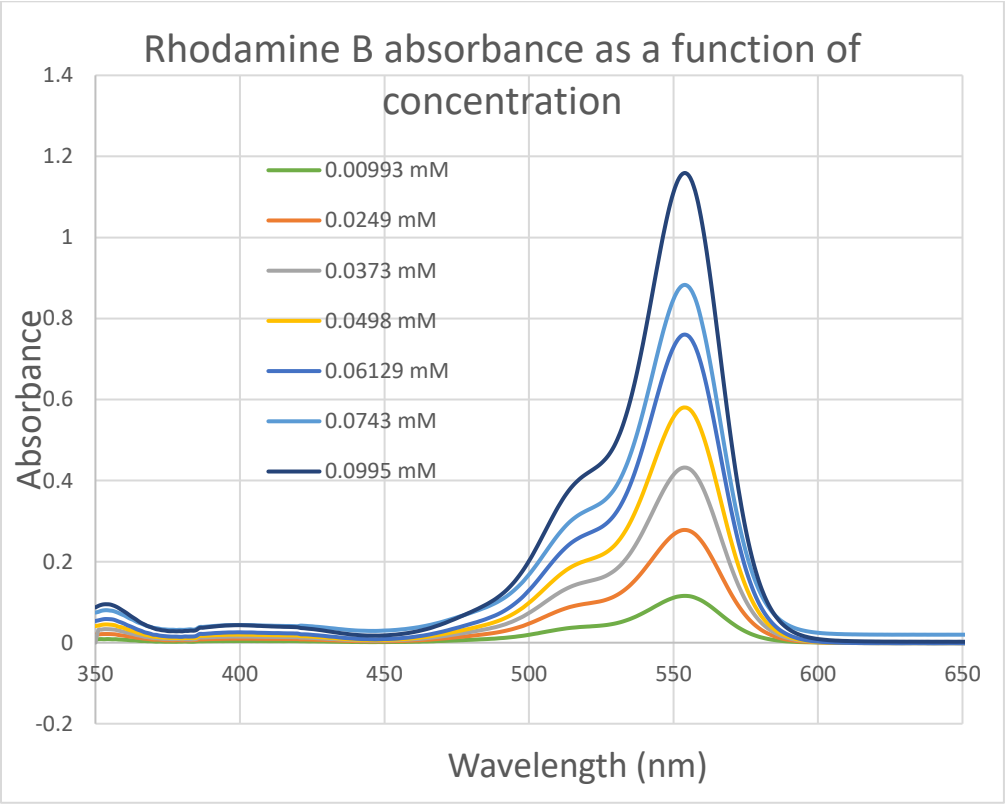

Figure 7: Absorbance spectra of Rhodamine B as a function of concentration

From this data, a Beer-Lambert plot was generated, and is shown in Figure 8. The gradient of this plot yields the molar absorption coefficient, which was found to 1.18×10^4.

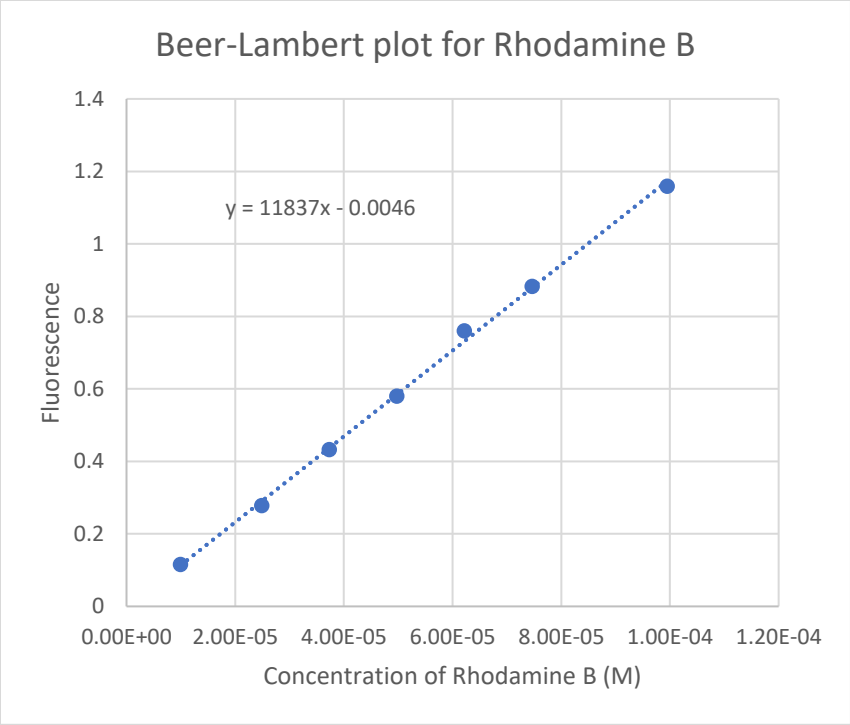

Figure 8: Beer-Lambert plot for Rhodamine B

The fluorescence spectra of 1 mM Rhodamine B before and after the addition of $CuSO_4$ are shown in Figure 9. The samples were excited at a wavelength of 500 nm. After adding 0.0581 g $CuSO_4$, the peak fluorescence intensity of Rhodamine B was reduced from an initial value of 125414 to 81070, or about 35.4% its initial value.

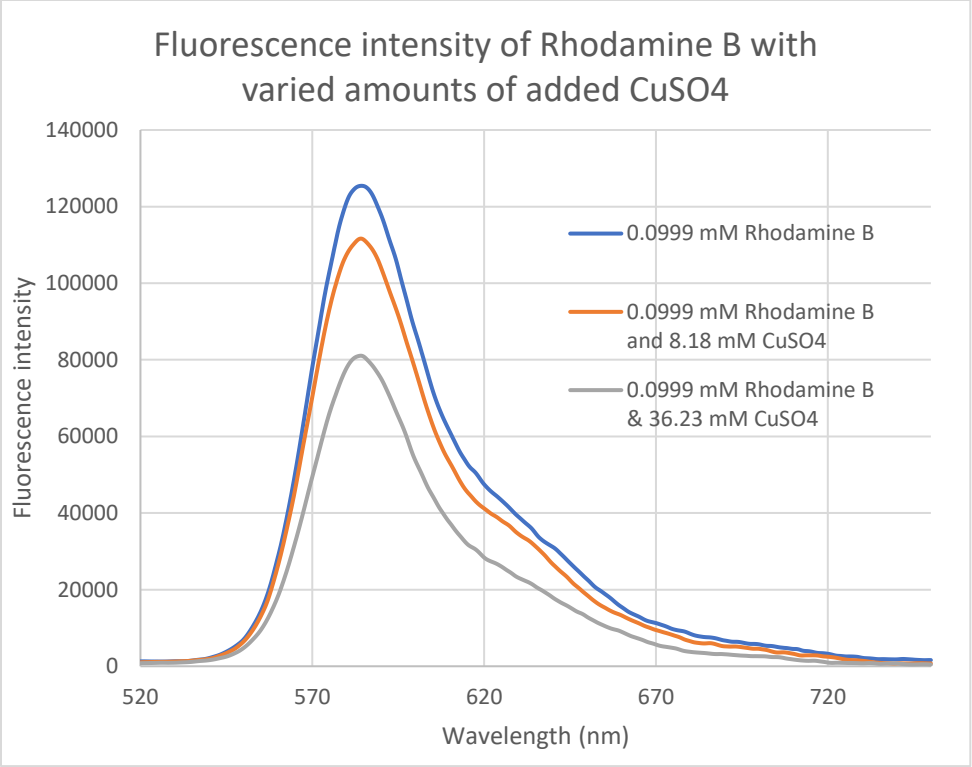

Figure 9: Changes in fluorescence intensity of Rhodamine B upon addition of $CuSO_4$

Figure 10 is a plot of the peak fluorescence of each solution with respect to the concentration of $CuSO_4$.

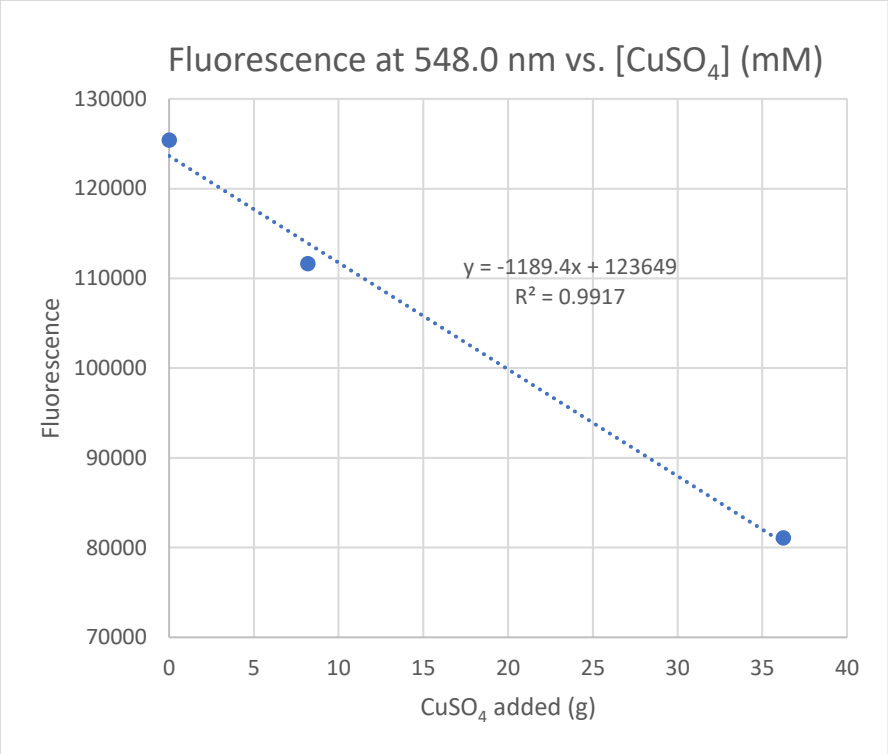

Figure 10: Change in fluorescence intensity of Rhodamine B with respect to concentration of $CuSO_4$

This plot was used to derive a numerical relationship between the concentration of copper (II) and the ion quenching of Rhodamine B. Using the Stern-Volmer relationship, the bimolecular quenching constant, k_q, was derived. Because k_q is dependent on the concentration of the quencher, $[Q]$, it was calculated for both concentrations of $CuSO_4$ observed.

At a $CuSO_4$ concentration of 8.18 mM, k_q was found to be 1.5085×10^{11} $M^{-}s^{-}$. When the $CuSO_4$ concentration was increased to 36.23 mM, k_q was found to be 1.5098×10^{11} $M^{-}s^{-}$.

Once k_q was derived, the fraction of excited states quenched was able to be estimated using:

$$fraction\ quenched = \frac{k_q[Q]}{k_d + k_q[Q]}$$

where k_d is equal to $1/\tau_0$. When the concentration of the quencher, $CuSO_4$ was 36.23 mM, it was estimated that the fraction of excited states quenched was approximately 5.44×10^{-3}.

Though the decrease in fluorescence does have a linear relationship to the concentration of $CuSO_4$, as was predicted, the rate of change was much less than desired. The fluorescence of pure Rhodamine B, which had an initial maximum of approximately 1.25×10^5, was only quenched by about 64.6% with the addition of $CuSO_4$ at a concentration approximately 363 times greater than that of the Rhodamine B. This is likely due to the short fluorescence lifetime of the dye, which limits the fraction of fluorescence that can be quenched. Because of this, Rhodamine B was eliminated as a candidate for the fluorophore.

3.2 Tris(2,2'-bipyridyl)dichlororuthenium(II) hexahydrate

In an attempt to find the most efficient quencher of $Ru(bpy)_3]^{2+}$ $2Cl^-$, five metal ion-containing solutions were tested. Figure 11 shows the effect that each metal had on the fluorescence of the $Ru(bpy)_3]^{2+}$ $2Cl^-$.

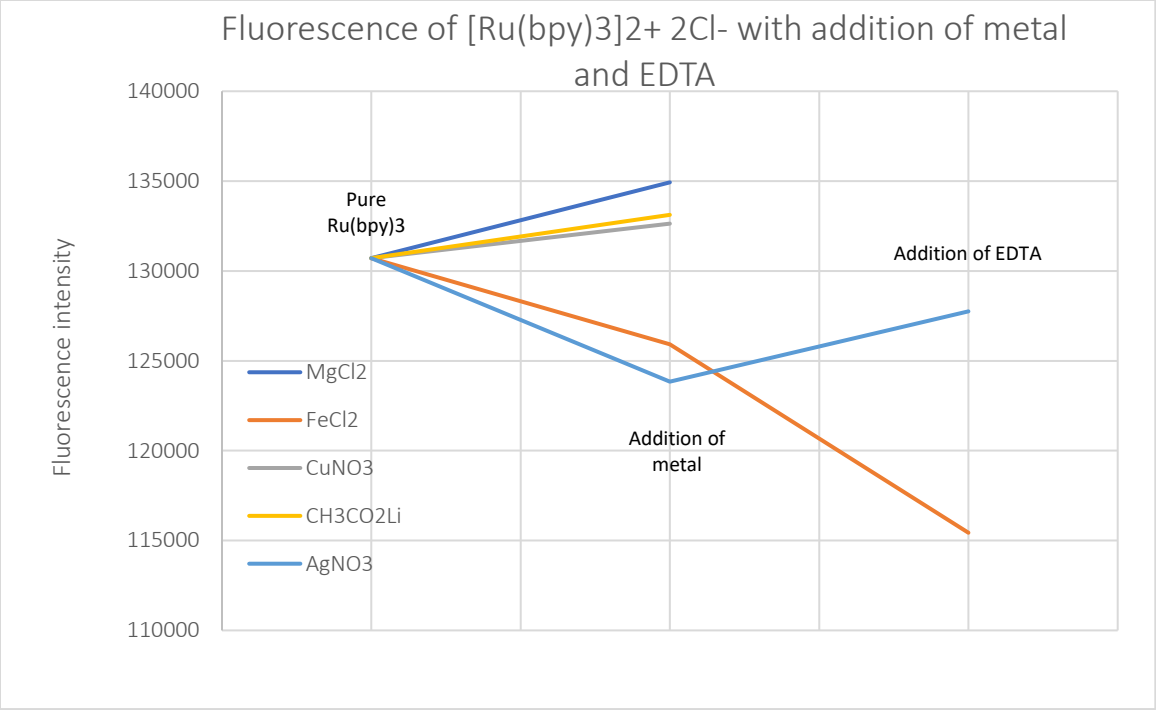

Figure 11: Changes in fluorescence intensity of $[Ru(bpy)_3]^{2+}$ with addition of metal complexes and EDTA

The first point shows the peak fluorescence of the pure $Ru(bpy)_3]^{2+}$ $2Cl^-$ solution. The second set of points, labeled "Addition of metal," shows the fluorescence intensity of the solution (in five separate cuvettes) after the addition of the metal solutions. Out of the 5 solutions, $AgNO_3$ and $FeCl_2$ quenched the fluorescence of the $Ru(bpy)_3]^{2+}$ $2Cl^-$. $MgCl_2$, $CuNO_3$, and CH_3CO_2Li all slightly increased the fluorescence of the dye, so they were eliminated as quencher candidates.

The third set of points on the graph shows the fluorescence intensity of the successfully quenched solutions after the addition of EDTA. When added to $FeCl_2$ solution, the EDTA further quenched the fluorescence. The addition of EDTA to the $AgNO_3$ solution partially restored its fluorescence intensity. This result led to further testing of $AgNO_3$.

The fluorescence spectra of a 0.09367 mM $[Ru(bpy)_3]^{2+}$ $2Cl^-$ solution before and after the addition of aliquots of $AgNO_3$ were recorded, as seen in Figure 12.

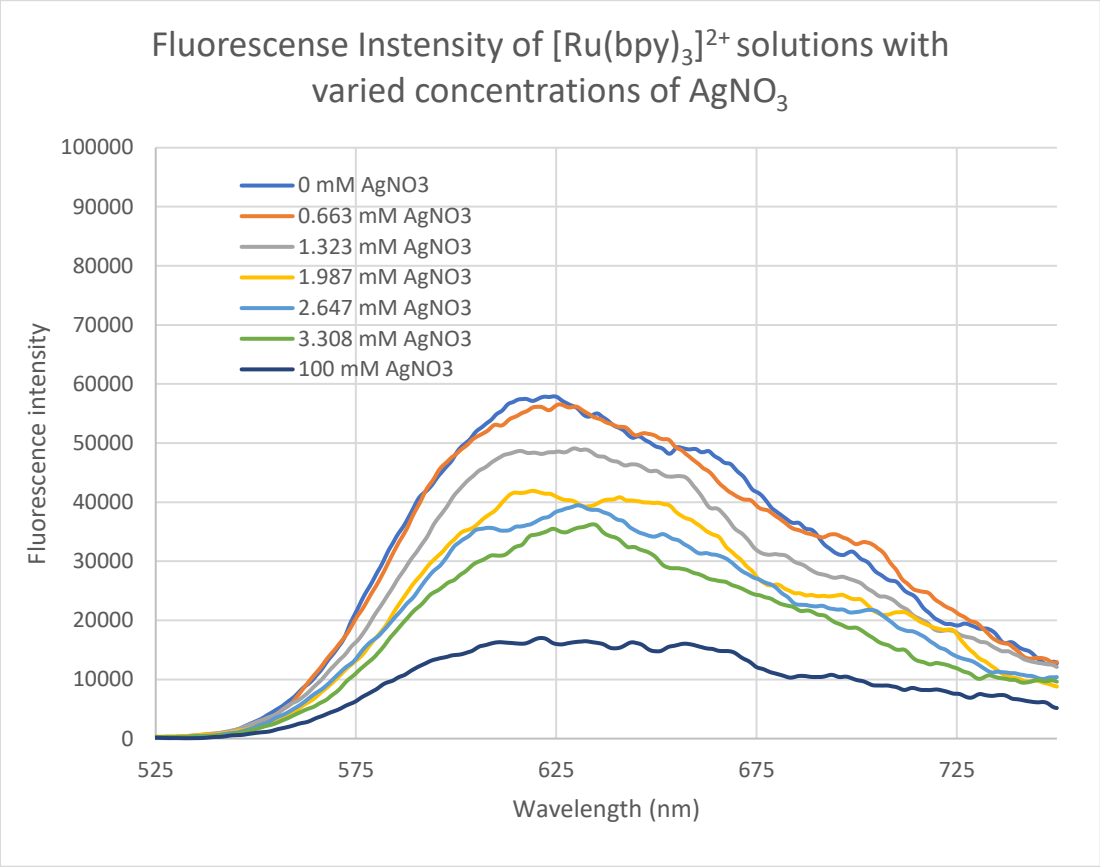

Figure 12: Fluorescence intensity of $[Ru(bpy)_3]^{2+}$ $2Cl^-$ solutions with varied concentrations of $AgNO_3$

When overlayed, these seven spectra clearly show a decrease in peak fluorescence intensity upon addition of $AgNO_3$. The peak fluorescence intensity of each solution was then plotted against the concentration of $AgNO_3$ to determine the numerical relationship between the concentration of $AgNO_3$ and the fluorescence quenching (Figure 13).

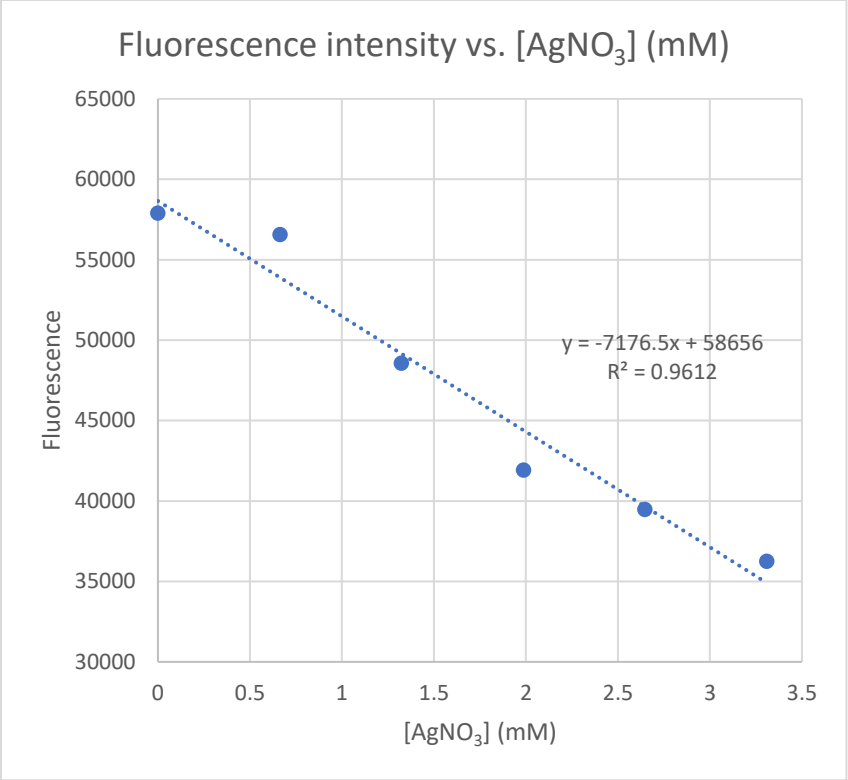

Figure 13: Changes in fluorescent intensity of $[Ru(bpy)_3]^{2+}$ with respect to concentration of $AgNO_3$

The absorbance of each sample was also plotted against the concentration of $AgNO_3$ and can be seen in Figure 14.

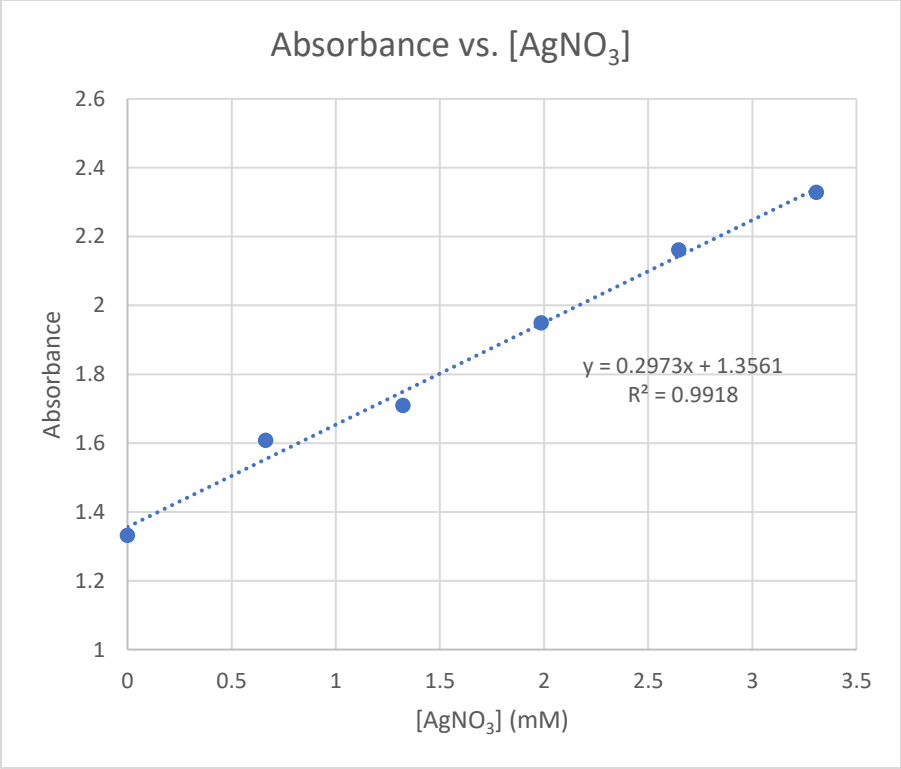

Figure 14: Changes in absorbance of $[Ru(bpy)_3]^{2+}$ with respect to concentration of $AgNO_3$

Compared to Rhodamine B and $CuSO_4$, $[Ru(bpy)_3]^{2+}$ $2Cl^-$ and $AgNO_3$ made a significantly more effective fluorophore-quencher pair. At a concentration about ten times less than the $CuSO_4$, the $AgNO_3$ was able to quench approximately 62.6% of the fluorescence of $[Ru(bpy)_3]^{2+}$ $2Cl^-$.

Next, to determine whether EDTA could consistently outcompete the $Ru(bpy)_3]^{2+}$ $2Cl^-$ and chelate the Ag (I), the fluorescence spectra of the $Ru(bpy)_3]^{2+}$ $2Cl^-$ and $AgNO_3$ solution were recorded before and after the addition of multiple aliquots of EDTA. When these spectra are overlayed, as in Figure 15, it is evident that there is no clear relation between the concentration of EDTA and fluorescence intensity.

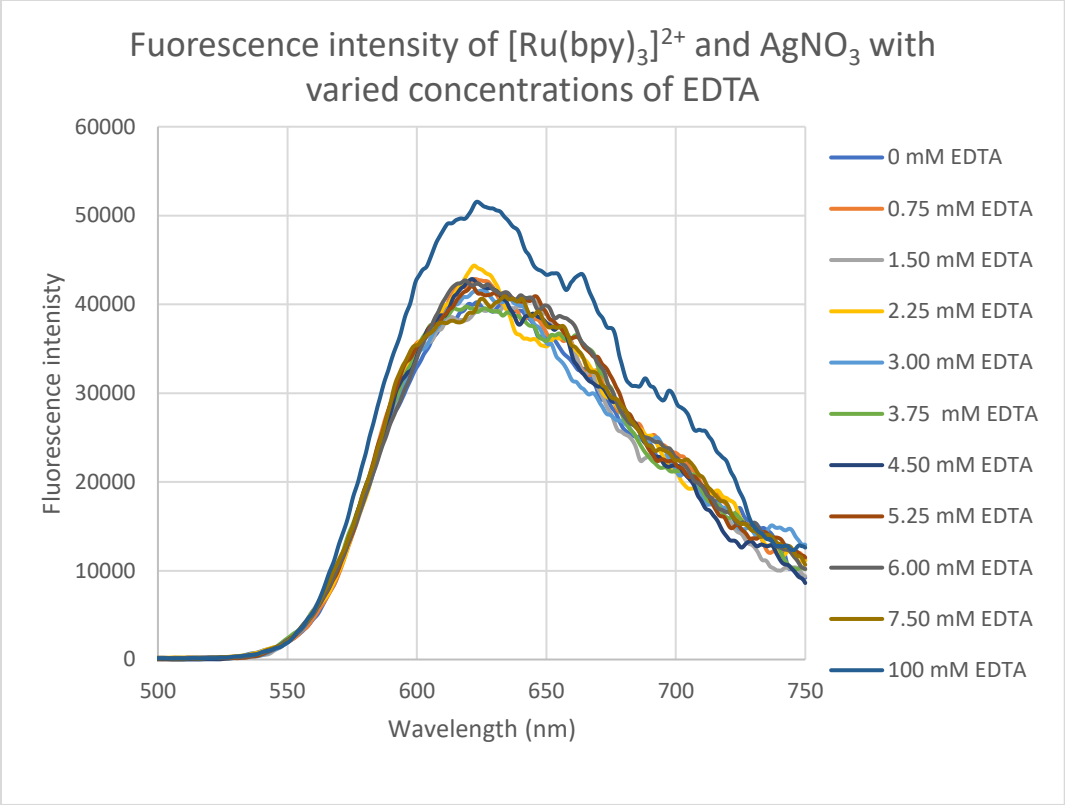

Figure 15: Spectra showing changes in fluorescence intensity of $[Ru(bpy)_3]^{2+}$ with respect to concentration of EDTA

Additionally, EDTA has the opposite effect on the fluorescence intensity as it did in the previous experiment. The first experiment showed an increase in fluorescence upon addition of EDTA, which was in line with the desired outcome. In this experiment, however, the addition of EDTA further decreased the fluorescence intensity. This shows that the EDTA was unable to consistently chelate the Ag (I) and remove it from the $Ru(bpy)_3]^{2+}$ $2Cl^-$.

Due to the unsuccessful results of this series of experiments, tests of $Ru(bpy)_3]^{2+}$ $2Cl^-$ were not continued.

3.3 Fluo-4FF

The peak fluorescence of the 1.74×10^{-7} mM Fluo-4FF solution was measured using 1, 2.5, and 5 nm slit widths. After the addition of each aliquot of $CaCl_2$, the peak fluorescence was recorded using 1 nm slit width, then a graph of fluorescence intensity versus concentration of $CaCl_2$ was created (Figure 16).

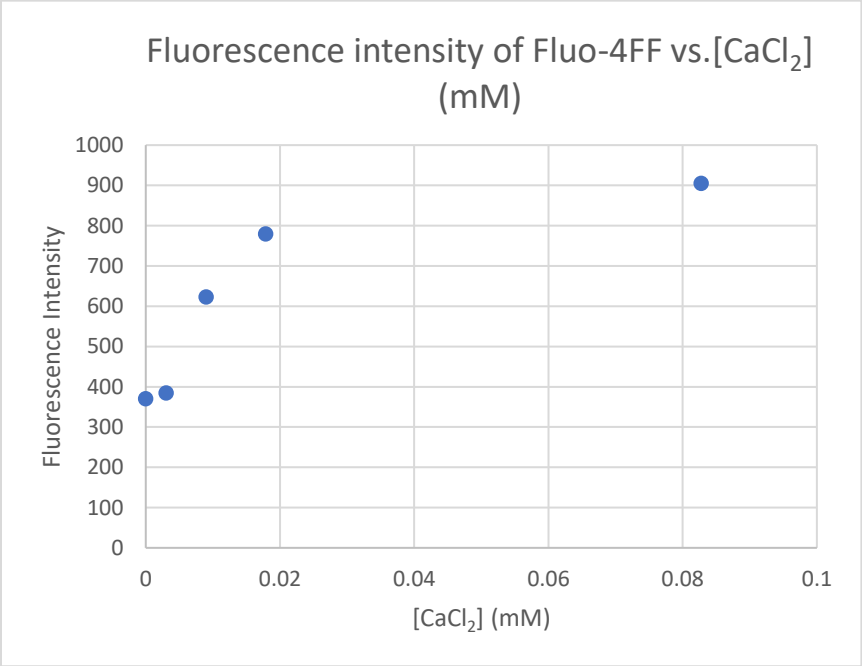

Figure 16: Change in fluorescence intensity of Fluo-4FF upon addition of $CaCl_2$

This plot does show the expected increase in fluorescence of Fluo-4FF, although the increase was not as dramatic as expected. The shape of the graph indicates that at a $CaCl^{2+}$ concentration of 0.01 mM, the dye reached its detection limits. Fluo-4FF is expected to exhibit a 100-fold increase in fluorescence upon binding Ca^{2+}, though in this experiment, the fluorescence intensity increased only by a factor of approximately 2.4.

After adding 300 µL of 10 mM EDTA to the sample, the peak fluorescence intensity was recorded. Figure 17 and shows the decrease in fluorescence intensity upon addition of EDTA.

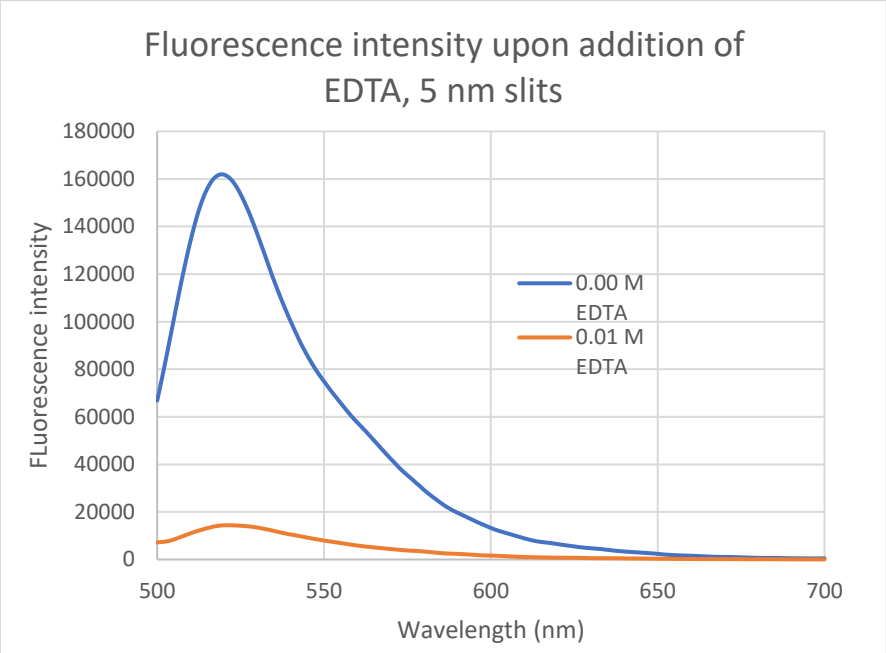

Figure 17: Spectra showing change in fluorescence intensity of Fluo-4FF upon addition of 300 uL EDTA,

The fluorescence decreased to 8.90% of its original intensity upon addition of EDTA. This major decrease in fluorescence in line with the predicted results of the experiment, despite the earlier unexpected behavior of the Fluo-4FF.

4.0 Discussion

Because of its prevalence in both pharmacological and non-pharmacological applications, there have been many studies done into the detection of EDTA. The goal of this study was to develop a method to determine EDTA concentration in samples based on the principles of fluorescence quenching and competition binding. Specifically, the research aimed to find a fluorophore-quencher pair that could be separated by the chelating ability of EDTA.

First, Rhodamine B and tris(2,2'-bipyridyl)dichlororuthenium(II) hexahydrate were tested as fluorophore candidates paired with various metals. These dyes are more commonly available and significantly less costly than the Fluo-4FF, which was tested later. Neither the Rhodamine B nor $[Ru(bpy)_3^{2+}]$ $2Cl^-$, however, yielded the desired results.

The fluorescence intensity of Rhodamine B was not able to be sufficiently quenched, even in the presence of excess quencher. This led to the abandonment of Rhodamine B as a possible fluorophore for the system. Conversely, the fluorescence of $[Ru(bpy)_3^{2+}]$ was able to be significantly quenched by a much lower concentration of metal ions. Upon addition of EDTA, there was not a significant increase in the solution's fluorescence, indicating that EDTA did not have a strong enough affinity for the metal ions to remove them from the fluorescent dye. After this point, $[Ru(bpy)_3^{2+}]$ was abandoned as well.

The final fluorophore, Fluo-4FF yielded the most successful results of the 3 dyes, despite initial concerns. The fluorescence intensity of Fluo-4FF typically increases by 100-fold in the presence of Ca^{2+}. In the experiment described in this paper, the fluorescence of the dye increased only by a factor of 2.4 upon addition of $CaCl_2$. Nonetheless, when enough EDTA was added to the

solution to bring it to a concentration of 0.01 mM, the fluorescence intensity was quenched by a by a significant factor. This result is extremely promising, as it shows that the EDTA was able to remove the Ca^{2+} from the Fluo-4FF, reversing the fluorescence increase.

Figure 17 displays the fluorescence spectra of Ca^{2+}-bound Fluo-4FF before and after the addition of EDTA. In the presence of EDTA, there was a 91.90% decrease in fluorescence intensity, compared to the initial intensities before addition of EDTA. The data obtained by measuring the fluorescence intensity of Fluo-4FF before and after the addition of EDTA can potentially be used to determine unknown concentrations of EDTA based on a calibration curve.

From a kinetic standpoint, it may be possible to predict the equilibrium concentrations of EDTA, Ca^{2+}, and calcium bound EDTA. The relation between EDTA, Fluo-4FF, and Ca^{2+} can be represented by

$$EDTA + [Ca\text{-}Fluo4FF] \rightleftharpoons EDTA + Fluo4FF + Ca^{2+} \rightleftharpoons [Ca - EDTA] + \quad Fluo4FF$$

The binding constant for EDTA and Ca^{2+} is 10^8 M, and the dissociation constant from Ca^{2+}-bound Fluo-4FF is about 10^{-5} m. The product of these equilibrium constants is 10^3, so it can be written that

$$K = 10^3 = \frac{[EC][F]}{[E][FC]}$$

$$\frac{[FC]}{[F_0] - [FC]} = \frac{[EC]}{10^3[E]}$$

$$\frac{[F_0]}{[FC]} - 1 = \frac{10^3[E]}{[EC]}$$

$$\frac{[F_0]}{[FC]} = \frac{10^3[E]}{[EC]} + 1$$

This shows that if the ratio of Ca^{2+}-bound EDTA to unbound EDTA could be calculated, it would be possible to determine how much of the Fluo-4FF was bound to Ca^{2+}.

4.1 Sources of error

Two main sources of error were identified after specific unexpected data and results were recorded. The errors are believed to come from contaminated deionized water, and incorrect choice of buffer. Before beginning these experiments, the pH of the deionized water used in experiments was measured and found to be 4.5, which is significantly more acidic than the expected pH of about 6. In an attempt to minimize any unwanted effects that the acidic water may have on the samples, all solutions from there on were made up using a KH_2PO_4 buffer with a pH of 7.2.

The use of a buffer was not fully effective in preventing unexpected results. The first indication of interference came during the testing of $[Ru(bpy)_3]^{2+}$ with $FeCl_2$ and EDTA. After successfully quenching the fluorescence of the dye with $FeCl_2$, the addition of EDTA should have either caused an increase in fluorescence intensity, or no change at all. Instead, the fluorescence decreased further, indicating that another reaction was taking place between the dye and ions not accounted for. At the time of this experiment, there was not yet a hypothesis as to where this may have been coming from.

The next indicator of interference appeared during the first tests of Fluo-4FF. This dye typically exhibits a 100-fold increase in fluorescence in the presence of Ca^{2+}. In a solution of 0.08 mM Ca^{2+}, the 1.74×10^{-7} mM Fluo-4FF only showed an increase in fluorescence intensity by a factor of about 2.4. There are two possibilities as to what may have caused this increase to be less than expected, and it is most likely that a combination of the two inhibited the fluorescence.

The first source comes from the inappropriate choice of KH_2PO_4 buffer used with a Ca^{2+} solution. The dissolved $CaCl_2$ and KH_2PO_4 react to produce soluble KCl and insoluble $Ca_3(PO_4)_2$. The precipitation of $Ca_3(PO_4)_2$ caused there to be fewer free Ca^{2+} ions in solution available to bind to the Fluo-4FF, decreasing the dye's signaling response. The second source is presumed to be contaminated DI water. Fluo-4FF has an affinity for other metal ions, such as Mg^{2+} and Fe^{2+}. Had these or other metal ions been present in the DI water, some of the Fluo-4FF would bind them instead of the Ca^{2+} and decrease the response signal.

As a final test, 3 mL of buffer and 20 μL Fluo-4FF (to give a concentration of 1.74×10^{-7}mM) were combined in a cuvette and the fluorescence intensity was measured and recorded. 300 μL EDTA were added to the cuvette and the fluorescence was remeasured. The results are shown below in Figure 18.

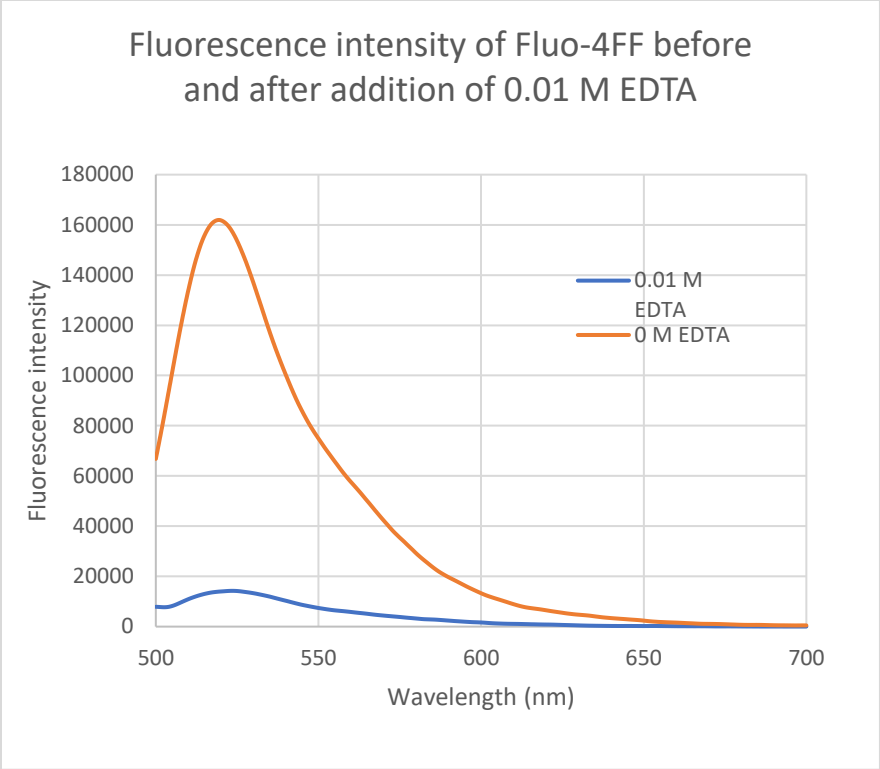

Figure 18: Fluorescence intensity of Fluo-4FF before and after addition of EDTA

Before the addition of EDTA, the peak fluorescence intensity of the Fluo-4FF was 161941, and after the addition of EDTA, it was reduced to 14242, only about 8.79% its original value. The addition of EDTA should not have caused this significant decrease in the fluorescence intensity. This result indicates that there were likely free metal ions in the deionized water, causing a reaction to occur other than that of EDTA and Fluo-4FF.

4.2 Future work

Further research and experimentation are required before this can be considered a viable method to detect EDTA concentrations. The tests carried out using Fluo-4FF should be improved and repeated to gather more thorough consistent results. A similar approach should be taken, first measuring the baseline fluorescence of a known concentration of Fluo-4FF, then adding $CaCl_2$ in

small aliquots and continuing to measure fluorescence intensity to assure that the dye is reacting as expected. EDTA should then be added gradually in known amounts to the sample, measuring the change in fluorescence after each addition.

From this data, a calibration curve should be plotted of fluorescence intensity versus EDTA concentration. The best fit line of this plot may be used to predict changes in fluorescence based on a corresponding concentration of EDTA added.

Going forward, it may be beneficial to choose a dye that is more sensitive to Ca^{2+}, as this process is reliant on a balance between affinities. A dye that can measure lower concentrations of Ca^{2+} is necessary. Because the affinity of EDTA for calcium is so high, there are relatively few free Ca^{2+} ions in solution that they dye can detect.

5.0 References

Albani, J. R. (2004). Chapter 4—Fluorescence Quenching. In J. R. Albani (Ed.), *Structure and Dynamics of Macromolecules: Absorption and Fluorescence Studies* (pp. 141–192). Elsevier Science. https://doi.org/10.1016/B978-044451449-3/50004-6

Bhattacharyya, S. N., & Kundu, K. P. (1971). Spectrophotometric determination of EDTA. *Talanta*, *18*(4), 446–449. https://doi.org/10.1016/0039-9140(71)80066-8

dos Santos, A. C., da Cunha, R., do Carmo Batista, W. V. F., de Fátima Gorgulho, H., & Benedini Martelli, P. (2023). Determination of EDTA in Aqueous Medium. *Proceedings of the National Academy of Sciences, India Section A: Physical Sciences*, *93*(1), 1–5. https://doi.org/10.1007/s40010-022-00788-7

Fluo Calcium Indicators. (2022). Molecular Probes. https://www.thermofisher.com/document-connect/document-connect.html?url=https://assets.thermofisher.com/TFS-Assets%2FLSG%2Fmanuals%2Fmp01240.pdf

George, T., & Brady, M. F. (2022). Ethylenediaminetetraacetic Acid (EDTA). In *StatPearls [Internet]*. StatPearls Publishing. https://www.ncbi.nlm.nih.gov/books/NBK565883/

Gentleman, A.S., Lawson, T., Ellis, M. G. Davis, M., Turner-Dore, J., Ryder, A.H.S., Frosz, M.H., Ciaccia, M., Reisner, E., Cresswell, A.J., & Euser, T.G. (2022). Stern–Volmer analysis of photocatalyst fluorescence quenching within hollow-core photonic crystal fibre microreactors. *Chemical Communications*, *58*(75), 10548–10551.

Griko, Y. V. (1999). Energetics of Ca2+–EDTA interactions: Calorimetric study. *Biophysical Chemistry*, *79*(2), 117–127. https://doi.org/10.1016/S0301-4622(99)00047-2

Hamano, T., Mistuhashi, Y., Tanaka, K., Matsuki, Y., Oji, Y., & Okamoto, S. (1985). Colorimetric determination of ethylenediaminetetra-acetic acid in foods. *Zeitschrift Fur Lebensmittel-Untersuchung Und -Forschung*, *180*(4), 280–283. https://doi.org/10.1007/BF01851269

Jarmoskaite, I., AlSadhan, I., Vaidyanathan, P. P., & Herschlag, D. (2020). How to measure and evaluate binding affinities. *ELife*, *9*, e57264. https://doi.org/10.7554/eLife.57264

Kalyanasundaram, K. (1982). Photophysics, photochemistry and solar energy conversion with tris(bipyridyl)ruthenium(II) and its analogues. *Coordination Chemistry Reviews*, *46*, 159–244. https://doi.org/10.1016/0010-8545(82)85003-0

Klippenstein, S. J., Pande, V. S., & Truhlar, D. G. (2014). Chemical Kinetics and Mechanisms of Complex Systems: A Perspective on Recent Theoretical Advances. *Journal of the American Chemical Society*, *136*(2), 528–546. https://doi.org/10.1021/ja408723a

Kristoffersen, A. S., Erga, S. R., Hamre, B., & Frette, Ø. (2014). Testing Fluorescence Lifetime Standards using Two-Photon Excitation and Time-Domain Instrumentation: Rhodamine B, Coumarin 6 and Lucifer Yellow. *Journal of Fluorescence*, *24*(4), 1015–1024. https://doi.org/10.1007/s10895-014-1368-1

Laidler, K. J., & Meiser, J. H. (1995). *Physical Chemistry* (2nd Edition). Houghton Mifflin Company.

Lakowicz, J. R. (Ed.). (2006). Mechanisms and Dynamics of Fluorescence Quenching. In *Principles of Fluorescence Spectroscopy* (pp. 331–351). Springer US. https://doi.org/10.1007/978-0-387-46312-4_9

Mottram, L. F., Forbes, S., Ackley, B. D., & Peterson, B. R. (2012). Hydrophobic analogues of rhodamine B and rhodamine 101: Potent fluorescent probes of mitochondria in living C.

elegans. *Beilstein Journal of Organic Chemistry*, *8*, 2156–2165. https://doi.org/10.3762/bjoc.8.243

Paris, J. P., & Brandt, W. W. (1959). CHARGE TRANSFER LUMINESCENCE OF A RUTHENIUM(II) CHELATE. *Journal of the American Chemical Society*, *81*(18), 5001–5002. https://doi.org/10.1021/ja01527a064

Rusak, D. A., James, W. H. I., Ferzola, M. J., & Stefanski, M. J. (2006). Investigation of Fluorescence Lifetime Quenching of Ru(bpy)32+ by Oxygen Using a Pulsed Light-Emitting Diode. *Journal of Chemical Education*, *83*(12), 1857. https://doi.org/10.1021/ed083p1857

Ryu, J., Nam, D. H., Lee, S. H., & Park, C. B. (2014). Biocatalytic Photosynthesis with Water as an Electron Donor. *Chemistry – A European Journal*, *20*(38), 12020–12025. https://doi.org/10.1002/chem.201403301

Sil, T. B., Sahoo, B., & Garai, K. (2018). Chapter Thirteen—Building, Characterization, and Applications of Cuvette-FCS in Denaturant-Induced Expansion of Globular and Disordered Proteins. In E. Rhoades (Ed.), *Methods in Enzymology* (Vol. 611, pp. 383–421). Academic Press. https://doi.org/10.1016/bs.mie.2018.08.027